The Journal of Neuroscience, November 1993, 13(11): 4889–4897

Differential Modulation of TTX-sensitive and TTX-resistant Na^+ Channels in Spinal Cord Astrocytes following Activation of Protein Kinase C

Chloe L. Thio and Harald Sontheimer

Department of Neurology, Yale University, School of Medicine, New Haven, Connecticut 06510

TTX-sensitive (TTX-S) and TTX-resistant (TTX-R) Na^+ currents are expressed in high densities (2–8 channels/μm^2) in astrocytes cultured from neonatal rat spinal cord. The two Na^+ current types differ up to 1000-fold in their TTX sensitivity and additionally have different steady-state activation (g–V) and inactivation (h_∞) curves. Expression of TTX-S and TTX-R Na^+ currents is confined to morphologically distinguishable subtypes of astrocytes, allowing characterization of the two types of Na^+ currents in isolation: *stellate cells* express TTX-S Na^+ currents and flat *pancake cells* express TTX-R Na^+ currents. Activation of protein kinase C (PKC) by phorbol 12-myristate 13-acetate (PMA) exhibited different effects on TTX-S and TTX-R Na^+ currents. PMA reduced peak TTX-S Na^+ currents by 25–60%; in contrast, PMA potentiated peak TTX-R Na^+ currents by 60–150%. These effects developed within minutes, and were typically not reversible. PMA effects were voltage dependent, and shifted steady-state Na^+ current activation of TTX-R and TTX-S currents by 6 and 18 mV, respectively, but without affecting their steady-state current inactivation (h_∞). PMA treatment also changed Na^+ current kinetics. TTX-R current activation (τ_m) was faster and current inactivation (τ_h) changed from a single- to a bi-exponential after PMA exposure, suggesting that PKC phosphorylation may have activated formerly quiescent Na^+ channels. In contrast, TTX-S current activation (τ_m) was unchanged, and current inactivation (τ_h), on average, decreased by 50% following PMA exposure. Since these effects of PMA could be reduced or abolished by the PKC inhibitor 1-(5-isoquinolinylsulfonyl)-2-methylpiperazine (H7), it is concluded that PMA effects were mediated by activation of PKC.

[Key words: TTX, Na^+ channel, phorbol ester, protein kinase C, astrocyte, patch clamp]

Protein phosphorylation is a fundamental regulatory mechanism in the control of membrane properties (Levitan, 1988) and is believed to be of major importance in modulating neuronal activity (Browning et al., 1985). Voltage-activated ion channels can be modulated by phosphorylation (Lemos et al., 1986; Levitan, 1988; Levitan et al., 1990) that can be mediated by a number of protein kinases (Lemos et al., 1986; Levitan, 1988; Levitan et al., 1990). Protein kinase C (PKC), in particular, has been demonstrated to be an abundant modulator of voltage-activated ion channels in neurons and other cells (Kaczmarek, 1987; Levitan, 1988; Levitan et al., 1990). For example, K^+ (Farley and Auerbach, 1986; Higashida and Brown, 1986; Malenka et al., 1986; Lotan et al., 1990), Cl^- (Madison et al., 1986), and Ca^{2+} (Rane and Dunlap, 1986) currents can be altered through PKC activation following exposure to phorbol esters or diacylglycerols (Nishizuka, 1984).

Two classes of Na^+ currents have been distinguished in neurons and muscle cells based on TTX pharmacology (Strichartz et al., 1987). TTX-sensitive (TTX-S) Na^+ currents are typically blocked by nanomolar concentrations of TTX, whereas TTX-resistant (TTX-R) Na^+ currents require micromolar concentrations of TTX for channel block (Kostyuk et al., 1981; Ikeda and Schofield, 1987; McLean et al., 1988; Schwartz et al., 1990; Caffrey et al., 1992; Roy and Narahashi, 1992). Molecular biology has further subclassified Na^+ channels, and has identified several members of a mammalian Na^+ channel multigene family. Those include several isoforms of TTX-S Na^+ channels expressed in neurons and muscle and at least two TTX-R Na^+ channels expressed in heart and denervated muscle (Noda et al., 1984; Barchi, 1987; Auld et al., 1988; Rogart et al., 1989; Cribbs et al., 1990; Kallen et al., 1990; see Catterall, 1988, for review). Using site-directed mutagenesis and subsequent expression of rat brain II Na^+ channel in *Xenopus* oocytes (Noda et al., 1989; Yang et al., 1992), it was possible to identify the amino acid residues that constitute the TTX-binding site of this TTX-S Na^+ channel. These studies strongly suggest that TTX-S and TTX-R Na^+ channels are distinct channel proteins.

Numerous phosphorylation sites have been identified on Na^+ channels from excitable cells (Costa et al., 1982; Catterall, 1988; Emerick and Agnew, 1989; Rossie and Catterall, 1989; West et al., 1991), and it has been suggested that they are of importance in regulating posttranslational events (Schmidt et al., 1985). Recently, one of the phosphorylation sites of the rat Na^+ channel α-subunits (a serine residue at position 1506 on the cytoplasmic loop between domains III and IV) was identified as a functional PKC modulation site for Na^+ channel activity (West et al., 1991). In this study (West et al., 1991) and others (Lotan et al., 1990; Dascal and Lotan, 1991; Numann et al., 1991), diacylgyceride, within minutes, decreased Na^+ currents in concert with a slowing of current inactivation. A similar reduction of Na^+ currents by the phorbol ester phorbol 12-myristate 13-

Received Jan. 25, 1993; revised May 3, 1993; accepted May 30, 1993.

We thank Drs. Mark Baker, James R. Howe, Bruce B. Ransom, and J. Murdoch Ritchie for helpful comments. This work was supported in part by the Eastern Paralyzed Veteran of America, EPVA (H.S.), and a fellowship from the American Heart Association (C.L.T).

Correspondence should be addressed to Harald Sontheimer, Ph.D., Department of Neurology, Yale University, School of Medicine, 333 Cedar Street, LCI 704, New Haven, CT 06510.

acetate (PMA) has previously been demonstrated in Na^+ channels expressed in *Xenopus* oocytes after injection of chick forebrain mRNA (Sigel and Baur, 1988). In all these studies, phorbol esters and diacylglycerides within minutes reduced Na^+ current amplitudes in concert with slowing Na^+ current inactivation.

In contrast to PKC effects on TTX-S Na^+ channels, little is known about the modulation of TTX-R Na^+ channels by protein kinase–mediated phosphorylation. We show here that PKC activation has different and opposite effects on TTX-S and TTX-R Na^+ currents expressed in spinal cord astrocytes: PKC activation by the phorbol ester PMA enhances currents mediated by TTX-R Na^+ channels, whereas it reduces currents mediated by TTX-S Na^+ channels. Furthermore, PKC effects on TTX-R Na^+ current kinetics are clearly distinct from those on neuronal and glial TTX-S Na^+ channels.

Materials and Methods

Cell culture. Cultures were obtained from neonatal Sprague–Dawley rats. Rat pups were deeply anesthetized by CO_2 narcosis and decapitated. Spinal cords between mid-cervical and lower lumbar levels were dissected free and the meninges removed. The cords were minced and incubated in an enzyme solution containing Earle's salts, 30 U/ml papain (Worthington), 0.5 mM EDTA, and 1.65 mM L-cysteine for 30 min at 37°C. The tissue was triturated in complete medium [Earle's minimal essential medium containing 10% fetal bovine serum (Hyclone), penicillin/streptomycin (500 U/ml each), and 20 mM glucose containing trypsin inhibitor and bovine serum albumin (BSA) (each 1.5 mg/ml)], and the cell suspension was plated onto polyornithine/laminin-coated 12 mm circular glass coverslips at a density of 2.5×10^5/ml. The cells were maintained at 37°C in a 5% CO_2, 95% air atmosphere and were fed every second day with complete medium. Recordings were obtained after 6–10 d. Glial fibrillary acidic protein staining shows that at this time cultures were >98% pure astrocytes. Cells from which recordings were obtained were identified morphologically: (1) *pancake cells* were round, non-process-bearing cells with large somata; (2) *stellate cells* had round, generally small somata and extensive processes that were often arborized. Their unique morphology made them easy to identify. Examples of the two cell types are displayed in Figure 1.

Electrophysiology. Methods for whole-cell current recordings were standard (Hamill et al., 1981) and used borosilicate glass pipettes (TW-150F-4, World Precision Instruments) containing (mM) *N*-methyl-D-glucamine, 120; tetraethylammonium chloride, 20; $MgCl_2$, 1; $CaCl_2$, 0.2; EGTA, 10; and HEPES (sodium salt), 10; pH was titrated to 7.4 with HCl (resistance was 3–5 MΩ); osmolarity of the pipette solution was 305 mOsm. Cells were continuously superfused with bath solution containing (mM) NaCl, 125; KCl, 5.0; $MgSO_4$, 1.2; $CaCl_2$, 1.0; Na_2HPO_4, 1.6; NaH_2PO_4, 0.4; glucose, 10.5; and HEPES (acid), 32.5; pH 7.4, 310 mOsm, adjusted with NaOH; which could be completely changed in less than 20 sec. PKC was activated using 1 μM phorbol 12-myristate 13-acetate (PMA; Sigma) added to the bath solution. PMA was diluted in a stock solution with dimethyl sulfoxide (DMSO; final DMSO concentration, 8 nM) and stored in aliquots at −20°C until use. To verify that effects of PMA were mediated by PKC, the PKC inhibitor H7 [1-(5-isoquinolinylsulfonyl)-2-methylpiperazine; 2 μM; RBI] was used added to the bath medium. H7 was dissolved in DMSO (final DMSO concentration, 8 nM) and stored in aliquots at −20°C. The concentration of H7 used was below the previously determined K_i of PKC inhibition (6 μM; Hidaka et al., 1984).

An Axopatch-1D amplifier (Axon Instruments), was used for recordings. Recordings were low-pass filtered at 3 kHz using an 8-pole Bessel filter (Frequency Devices), and were digitized on line at 100 kHz using a Labmaster TL-125 digitizing board (Axon Instruments). Data acquisition, storage, and analysis were performed using pCLAMP (Axon Instruments). For all measurements, capacity compensation (C_p) and series resistance compensation (R_s) were used to their full extent to minimize voltage errors; optimal settings for C_p and R_s were obtained by minimizing the capacity transient in response to a hyperpolarizing voltage step. R_s compensation was set to values of >80% in all recordings, and recordings were only used in which R_s was <10 MΩ before activating R_s compensation. Residual errors were calculated to be less than 5% of the command voltage, and traces were not corrected for these residual errors. Only recordings that met the following criteria were included in our analysis: (1) series resistance before compensation of errors was <10 MΩ; (2) Na^+ currents reached their peak within <800 msec; (3) Na^+ currents reversed within 5–10 mV of the mean current reversal potential, which was close to the theoretical equilibrium potential for Na^+. On-line leak subtraction was performed during recordings using a *P*/4 protocol (Bezanilla and Armstrong, 1977). All recordings were obtained at room temperature, typically 22°C. In all recordings that involved subsequent drug application, whole-cell capacitance and series resistance were continuously monitored. Only such recordings in which both parameters did not change by more than 10% were evaluated.

Step protocols. Two step protocols were used to activate Na^+ currents and to determine the voltage dependence of steady-state activation and steady-state inactivation h_∞, respectively.

(1) The protocol to study current activation stepped the membrane from a prepulse potential of −110 mV for 10 msec to potentials ranging from −70 to 80 mV in 10 mV increments. Time between steps was 2 sec, during which cells were held at −80 mV, and prepulses were applied for 200 msec. Conductance–voltage (*g–V*) curves were constructed from the resulting currents by determining the peak current for each potential, and converting current to conductance by dividing it by $V_m - E_{Na^+}$, whereby current reversal potential was considered E_{Na^+}. The resulting conductance values were plotted as a function of step potential to yield *g–V* curves.

(2) Steady-state inactivation was determined by varying the prepulse potential, at which cells were held for 200 msec, from −160 mV to −30 mV in 10 mV increments, and currents were then activated by a 10 msec step to 0 mV. Time between steps was 2 sec. Peak currents were determined for each prepulse potential, and these were normalized to the largest current recorded (typically at <−130 mV). This yielded normalized currents I/I_{max}, which were plotted as a function of prepulse potential to yield h_∞ curves.

Data analysis and curve fitting. Data analysis was performed on leak-subtracted current traces, after *P*/4 leak subtraction had been obtained (Bezanilla and Armstrong, 1977). Analysis of digitized data traces and curve fitting to those traces as well as fitting to cumulative data were done using the script interpreter of a scientific plotting program (ORIGIN, MicroCal Inc.). All these fits were obtained using a Marquard-Levenberg nonlinear-squares algorithm. The models and equations to which sets of data were fit are given below. Cumulative data analysis was performed by exporting measures obtained with CLAMPAN (Axon Instr. Inc.) to a spreadsheet (EXCEL) and computing statistical values (mean, SD, SEM) for spreadsheet data. These values were exported for graphing and curve fitting to the same plotting program (ORIGIN, MicroCal) used for analysis of digitized data. Time constants for current activation and inactivation were obtained by fitting data to the empirically derived Hodgkin–Huxley model (Hodgkin and Huxley, 1952). Current kinetics were described by an $m^p h$ model. Na^+ currents were converted to conductances by dividing digitized traces point by point by $V_m - E_{Na^+}$. Current reversal potential was considered to be E_{Na^+}. The derived Na^+ conductances were fit by the following equation representing the Hodgkin–Huxley model:

$$f(t) = A_0 + A_1 \cdot (1 - \exp(-(t - t_0)/\tau_m))^p \cdot (\exp(-(t - t_0)/\tau_h)),$$

where A_0 and A_1 were amplitude factors, t_0 was a time (offset) factor, and τ_m and τ_h were the time constants for activation and inactivation, respectively. p was the power factor for the activation (m) term and was set to 3 for pancake cells and 4 for stellate cells (see Sontheimer and Waxman, 1992b, for details).

In those instances where superimposed and scaled conductance traces were compared (e.g., Fig. 7), τ_h values were obtained from fitting the decay phase of Na^+ currents. In these instances the data was fit to exponentials of the form

$$f(t) = A_1 \cdot \exp(-(x - x_0)/\tau_1) + A_2 \cdot \exp(-(x - x_0)/\tau_2).$$

Steady-state inactivation curves (h_∞; see Fig. 6) and conductance–voltage (*g–V*) curves (see Fig. 5) were fit to a modified Boltzmann equation of the form

$$h(V) = 1/[1 + \exp((V - V_{1/2})/a)],$$

with $V_{1/2}$ representing the midpoint and a representing the slope factor of the sigmoidal curve.

Statistics. All cumulative data were given as mean ± standard error (SD) and were graphed as mean ± standard error of mean (SEM), with error bars representing SEM. Significance testing was done using either *t* test or Mann–Whitney (Wilcoxon) test depending on distribution of

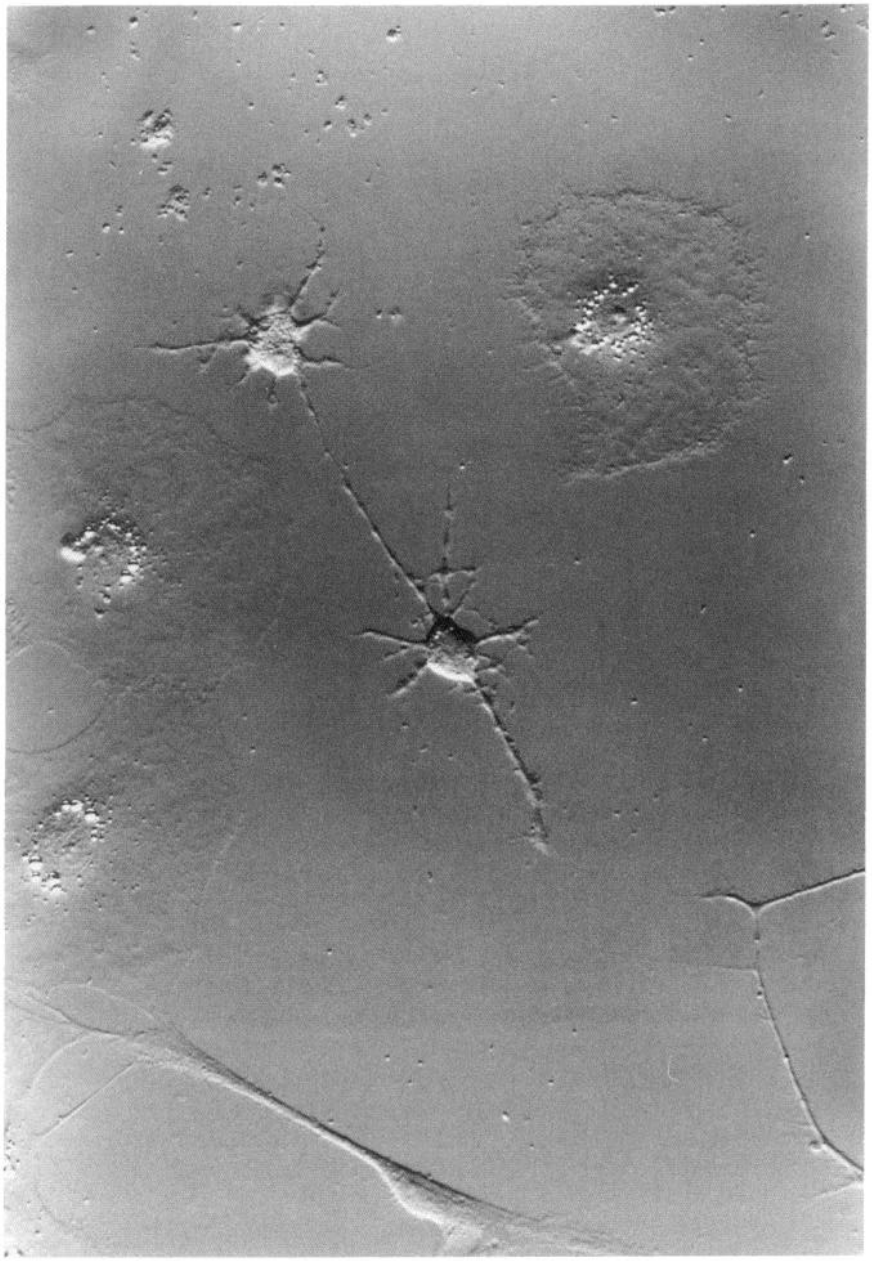

Figure 1. Cultures of postnatal day 0 rat spinal cord contain up to five different morphological subtypes, of which two are easily distinguishable morphologically, and three others are highly variable. Representative examples of the two unequivocal cell morphologies are demonstrated: *stellate*, process-bearing astrocyte cell and non-process-bearing *pancake* cell. Recordings were obtained from cells that were identified morphologically as either stellate or pancake cells. These two cell types were chosen for study because they selectively express different forms of Na^+ currents: stellate cells express TTX-S Na^+ currents; pancake cells express TTX-R Na^+ currents.

data. Student's *t* test for independent, unpaired variables was used whenever the data followed a Gaussian distribution. A two-sided Mann–Whitney (Wilcoxon) test was employed for data sets with non-Gaussian distribution.

Results

In studying modulatory effects of PKC activation on Na^+ currents, we took advantage of our recent observation that cultured spinal cord astrocytes express voltage-activated Na^+ channels in relatively high densities (2–8 channels/μm^2; Sontheimer et al., 1992), comparable to Na^+ channel densities of cultured neurons (Catterall, 1984; MacDermott and Westbrook, 1986). As previously described for astrocytes cultured from hippocampus (Sontheimer et al., 1991), cerebellum (Dave et al., 1991; Wyllie et al., 1991), or optic nerve (Raff, 1989), spinal cord cultures contain two easily distinguishable types of astrocytes: flat, non-process-bearing *pancake cells* and process-bearing *stellate cells* (Fig. 1) (Miller and Szigeti, 1991; Black et al., 1993). Na^+ currents in stellate cells express TTX-S Na^+ currents (K_d = 5.7 nM) with kinetic features similar to most cultured neurons. Pancake astrocytes, in contrast, exclusively express TTX-R Na^+ currents (K_d = 1000 nM) with 25 mV more hyperpolarized h_∞ and m_∞ curves (Sontheimer and Waxman, 1992b). Unlike dorsal root ganglion neurons, which can express both TTX-R and TTX-S channels within the same cell (Kostyuk et al., 1981; Roy and Narahashi, 1992), the two forms of Na^+ currents are confined to distinct subpopulations of spinal cord astrocytes, allowing the study of each current in isolation. Thus, this preparation was ideally suited to study and compare the modulatory influences of PKC activation on TTX-S and TTX-R Na^+ currents.

Examples of TTX-S and TTX-R Na^+ whole-cell currents recorded in the presence (PMA, continuous lines, Fig. 2*a,c*) and absence (control, dotted lines, Fig. 2*a,c*) of 1 mM PMA dem-

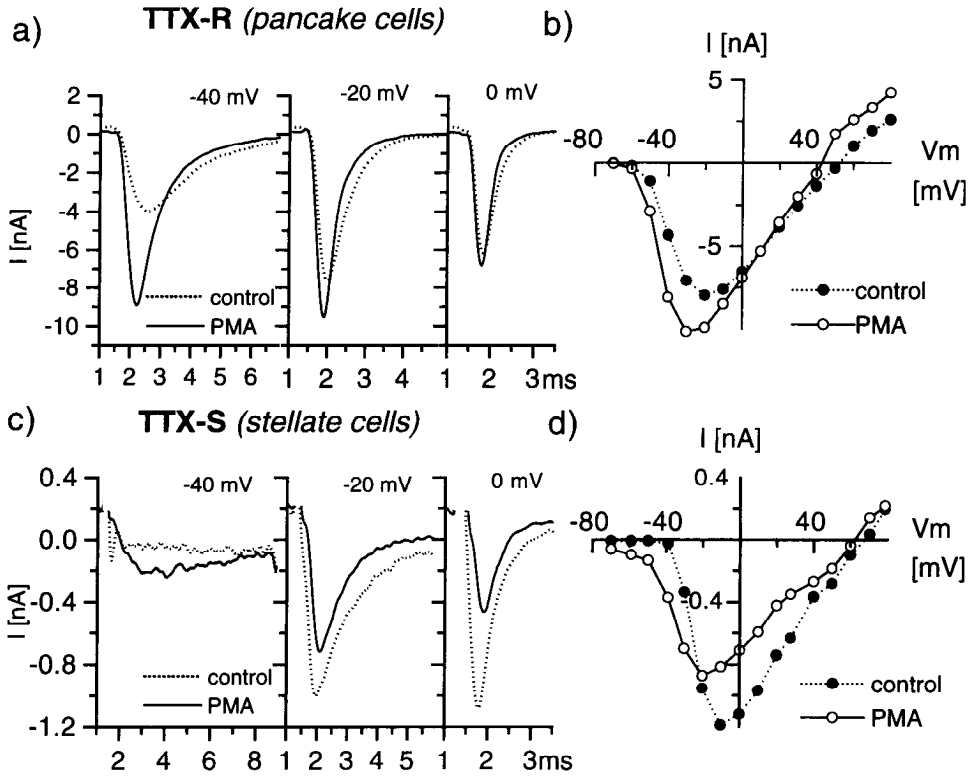

Figure 2. PMA effect on TTX-R and TTX-S Na^+ currents. Representative recordings from a pancake cell expressing TTX-R Na^+ currents (*a, b*) and a stellate cell expressing TTX-S Na^+ currents (*c, d*). Exposure to 1 μM PMA within 5 min increased peak TTX-R currents (*a*) and at potentials close to threshold (−40 mV) more than doubled currents as compared to control (*dotted lines*). PMA effect on TTX-R currents was voltage dependent and decreased with increasing voltage (*b*). Currents were almost unaffected at potentials > 0 mV (*a, b*). The peak of the *I–V* curve was shifted by about −10 mV. PMA affected TTX-S currents in the opposite way, and led to a reduction of peak currents at most potentials (*c, d*). Only at potentials close to threshold (*c*; −40 mV) were currents slightly increased by PMA. PMA effect was largest at potentials close to the peak (*d*; −10,0 mV). The peak of the *I–V* curve shifted by 10 mV in PMA (*d*).

onstrate that both current types are sensitive to PMA. Effects on TTX-R (Fig. 2*a,b*) and TTX-S Na^+ currents (Fig. 2*c,d*) differ in both the direction of PMA-induced modulation (enhancement vs reduction) and their voltage dependence. The latter is most visible when comparing current–voltage curves constructed from peak Na^+ currents before (continuous lines, Fig. 2*b,d*) and after (dotted lines, Fig. 2*b,d*) PMA application. PMA typically reduced peak current amplitude of TTX-S Na^+ currents and shifted the peak of the *I–V* curve, whereas it potentiated TTX-R Na^+ currents and resulted in a positive shift of the *I–V* curve peak (voltage dependence was analyzed in more detail below). TTX-R current potentiation was most notable at potentials between −50 mV and −20 mV, which is close to the Na^+ current activation threshold, and at more positive potentials PMA enhancement was barely visible or absent (Fig. 2*a,b*). Similarly, at potentials close to threshold (−40 to −30 mV), TTX-S Na^+ currents were enhanced by PMA, whereas in contrast to TTX-R Na^+ currents, PMA reduced peak TTX-S currents at all other potentials. This effect was most pronounced at potentials more positive than −20 mV (Fig. 2*c,d*).

These effects of PMA on Na^+ currents developed rapidly, and were always detectable after 3–5 min of drug exposure (Fig. 3). PMA-induced reduction of TTX-S Na^+ currents reached steady-state levels after 5 min and, on average, reduction of peak currents, determined in response to voltage steps to −10 mV, was 30% (SD, 18.9 %; $N = 22$; Fig. 3*a,c*). Similarly, PMA potentiation of TTX-R Na^+ currents was detectable after 3–5 min (Fig. 3*c*) and reached steady-state levels after 15 min, when the average potentiation, determined in response to voltage steps to −30 mV, was 94% (SD, 65.6%; $N = 22$). PMA effects did not increase further with longer exposures (not shown; $N = 5$ for both current types). To assure that these changes were not related to unspecific loss or gain of active Na^+ channels, control values yielding baseline current amplitudes were obtained for at least 6 min ($N = 12$) but up to 15 min ($N = 10$) prior to PMA application (Fig. 3*c*). Furthermore, 20 cells not treated with PMA and recorded for at least 30 min did not show significant changes in current amplitudes (range, 94–105% of control).

The modulation of Na^+ currents by PMA was almost irreversible. The potentiation of TTX-R Na^+ currents by PMA, on average, recovered by less than 20% of control following a 10–30 min wash (Fig. 4*a*). The recovery of TTX-S current suppression by PMA was even slower and less complete, and recovery never exceeded 10% of control after a 10 min wash (Fig. 4*b*). The traces illustrated in Figure 4 are representative examples of 22 recordings each for both current types, and both show little to no recovery from PMA ($N = 22$ each).

Although phorbol esters, such as PMA used in this study, are well-established activators of PKC and are frequently used as tools to induce PKC activation (Nairn et al., 1985; Sigel and Baur, 1988), direct effects of phorbol esters on ion channel activity not involving PKC activation cannot be excluded, particularly since such direct effects on ion channels were observed with diacylglycerides (Hockberger et al., 1989). To demonstrate that PMA effects on TTX-S and TTX-R Na^+ channels in spinal cord astrocytes were mediated by PKC activation rather than directly affecting their Na^+ channels, we studied PMA effects in the presence of 1-(5-isoquinolinylsulfonyl)-2-methylpiperazine (H7), a widely used PKC inhibitor (Hidaka et al., 1984). A 5 min pretreatment of cells with 2 μM H7 significantly reduced, and often abolished, PMA effects on both TTX-S and TTX-R currents (Fig. 5*a,c*), suggesting that these effects of PMA on Na^+ currents were mediated by PKC. The inhibitory action of H7 was reversible, and after a 5 min wash, PMA in the absence of H7 showed effects similar to those observed previously under control conditions (Fig. 5*a,c*, last trace; compare to Fig. 3*a,b*).

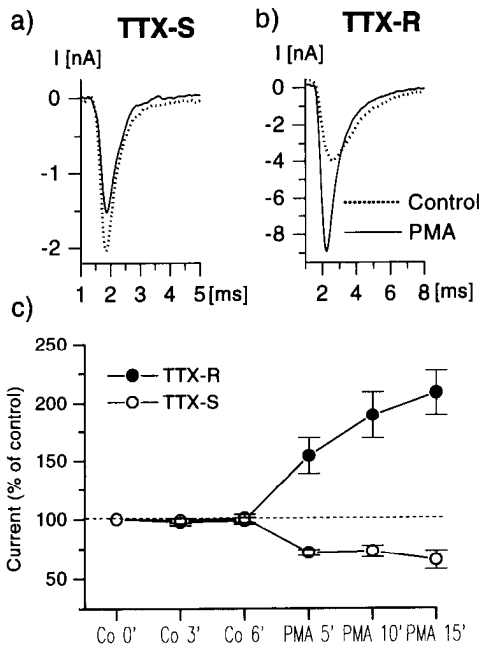

Figure 3. Time course of PMA effects. The time course of PMA effects on TTX-S and TTX-R currents was assessed in 22 experiments each; example traces are shown in *a* and *b*, and mean changes in peak currents are plotted as a function of time in *c* (error bars = SEM). PMA effect was normalized to control amplitudes that were obtained for 6–15 min (only up to 6 min shown) in standard solution (*Control, dotted line*) representing 100% effect. Due to the voltage dependence of PMA effects (Fig. 2) maximal effects were determined at −10 mV for TTX-S Na^+ currents and at −30 mV for TTX-R currents. PMA, within 5 min, decreased TTX-S current amplitudes by 25% (*a, c, open circles*) and effects were largest at 15 min (30%). TTX-R currents increased by 94–194% of control within 15 min (*b, c*).

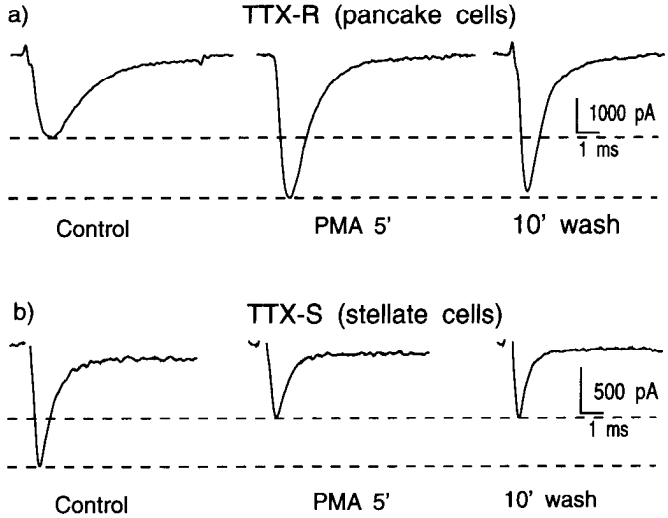

Figure 4. PMA effects are not reversible. Current recordings were obtained in the absence (*Control*) and presence (*PMA*) of PMA, and voltage steps displayed to activate Na^+ currents were −30 mV for TTX-R Na^+ currents (*a*) and −10 mV for TTX-S Na^+ currents (*b*). The reversibility of PMA-induced changes was studied by following Na^+ currents for up to 30 min after PMA has been washed out of the bath. Complete bath exchange was completed after 20 sec. PMA-induced changes in current amplitude showed little reversibility for both TTX-R (*a*) and TTX-S (*b*) currents ($N = 22$ each).

Since we observed that PMA effects were voltage dependent, apparent changes in peak currents at a given voltage could be due to shifts in steady-state current kinetics. Thus, we studied the voltage dependence of PMA effects in more detail, and constructed conductance–voltage (g–V) curves (Fig. 6) and steady-state inactivation (h_∞) curves (Fig. 7) for both current types in the presence and absence of PMA (see Materials and Methods for step protocols and fitting routines used). Conductance values were obtained by dividing whole-cell currents point by point by the driving force $V_m = V_{step} - E_{Na^+}$, and these values were then normalized to the peak conductance value. Conductance–voltage curves were constructed from mean conductances of five cells expressing TTX-S and five cells expressing TTX-R Na^+ currents. These g–V curves were plotted in two differing ways in Figure 6. In Figure 6, *a* and *b*, conductances were normalized to the largest conductance observed, and illustrate the relative difference in conductances in the presence and absence of PMA. Thus, PMA strongly reduced TTX-S Na^+ conductances at all potentials more positive than −20 mV (Fig. 6*a*), whereas it enhanced TTX-R Na^+ conductances at all potentials (Fig. 6*b*). To determine PMA-induced changes in the voltage dependence, additional g–V curves were plotted in which conductances were each normalized to the largest conductance (Fig. 6*c,d*), and these normalized g–V curves demonstrate that PMA, within 5 min, shifted the g–V curves of TTX-S and TTX-R Na^+ currents by 18 mV (TTX-S, $N = 5$) and 6 mV (TTX-R, $N = 5$), respectively (Fig. 6*c,d*). These shifts both were statistically significant ($p < 0.05$). It is evident that, in both current types, this negative shift of the activation curve leads to increased peak currents at potentials < −30 mV and shifts the threshold for current activation toward more negative potentials. This negative shift was rather small for TTX-R Na^+ currents and cannot fully account for the large degree of current potentiation observed (mean increase, 94%) at potentials between −50 and −20 mV. The comparatively large shift by PMA in the g–V curves observed for TTX-S currents, on the other hand, should, in the absence of any other effects, lead to enhanced peak currents at potentials between 0 and −60 mV. This was, however, only observed at threshold potentials, for example, close to −40 mV (see Fig. 2*c*, left trace) where small inward currents were discernible only after PMA exposure, whereas at more positive potentials current amplitudes decreased.

In contrast to these changes in current activation, steady-state inactivation (h_∞) curves for TTX-R and TTX-S Na^+ currents showed little change in PMA (Fig. 7*a,b*). A small (3–6 mV) negative shift was observed for both current types, and this shift was not statistically significant ($p = 0.22$ for TTX-R; $p = 0.81$ for TTX-S). Similar shifts in h_∞ curves are frequently observed with progression in time of whole-cell recordings and have been related to a loss of cytoplasmic constituents associated with cell dialysis in whole-cell recordings (Marty and Neher, 1983).

Since effects of PKC on inactivation kinetics of neuronal Na^+ channels have been reported, we investigated whether PMA produced an effect on the time constant of current activation (τ_m) or inactivation (τ_h) of astrocytic Na^+ currents. Such differences are easily visualized when Na^+ conductances obtained before and after PMA exposure are normalized to the same scale, and then superimposed. Representative examples of this are displayed in Figure 8. For TTX-S Na^+ currents (Fig. 8*a*), the time to peak (indicated by arrows) was similar for control and after PMA treatment, indicating that τ_m probably did not change. By contrast, TTX-R Na^+ currents are activated and peak more rapidly after PMA treatment as compared to control

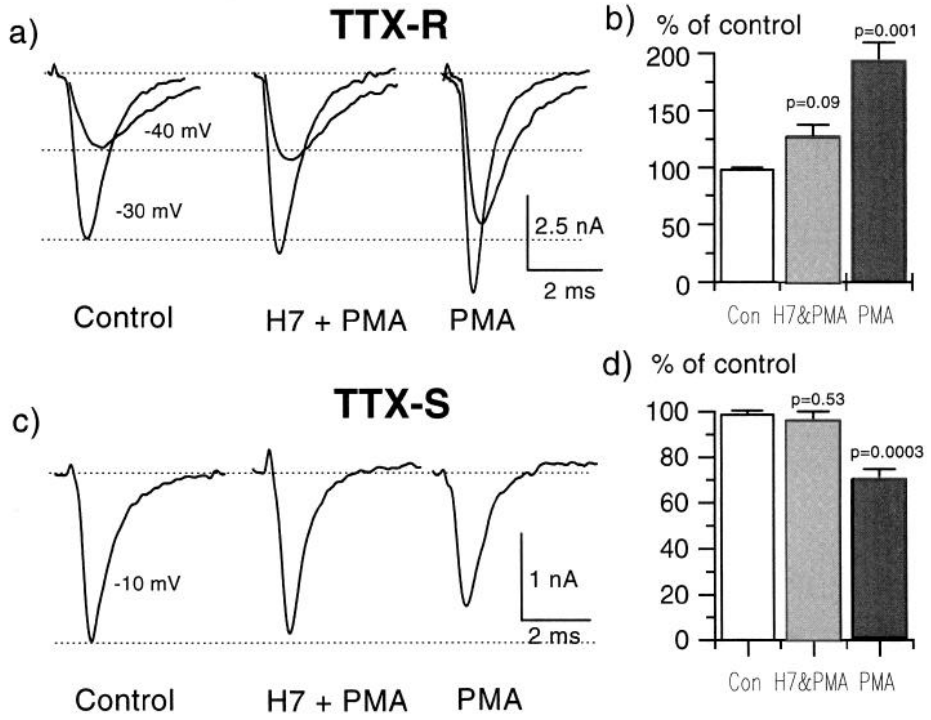

Figure 5. PMA effect can be inhibited by the PKC inhibitor H7. To show that PMA effects on Na^+ currents are mediated by activation of PKC, PMA effects were recorded in the presence and absence of the PKC inhibitor H7 [1-(5-isoquinolinylsulfonyl)-2-methylpiperazine; 2 mM, RBI] added to the bath medium. In both TTX-R (*a*) and TTX-S (*c*) currents, effects of PMA were strongly reduced in the presence of H7 (*H7+PMA*) as compared to PMA effects alone (*PMA*), and were comparable to control recordings prior to drug application. Exposure to PMA alone, after 10 min wash following H7 treatment, exerted normal PMA effects on TTX-R and TTX-S currents (*a, c, PMA*), thus demonstrating that PMA effects are mediated by activation of PKC. In *b* and *d*, mean effects of PMA and of PMA plus H7 are graphed for seven cells studied (error bars = SEM) for TTX-R and TTX-S Na^+ currents, respectively. PMA effects in the presence of H7 were not significantly different from control, but PMA effects in the absence of H7 were highly significant.

(Fig. 8*b*, arrows), indicating that in PMA τ_m may have decreased. Despite limitations in fitting fast, transient events accurately, we attempted to fit τ_m before and after PMA treatment using the empirically derived Hodgkin–Huxley equation (see Materials and Methods). These fits yielded values for τ_m of 0.17 ± 0.06 msec and 0.24 ± 0.11 msec for control and after PMA treatment, respectively ($p = 0.19$, $N = 6$ at −10 mV), in TTX-S Na^+ currents, and values of 0.36 ± 0.14 msec and 0.24 ± 0.05 msec (at −30 mV, $N = 6$, $p < 0.05$) for control and PMA data, respectively, in TTX-R Na^+ currents. Thus, the values derived from fitting data support the notion that PMA reduces τ_m of TTX-R Na^+ currents but does not affect τ_m of TTX-S Na^+ currents.

In addition, the superimposed traces allow qualitative assessment of alteration in current inactivation, and demonstrate that for both TTX-S and TTX-R Na^+ currents inactivation is more rapid after PMA exposure than under control conditions. The time constant for current inactivation τ_h can be derived more accurately than τ_m by either fitting the current decay phase only to an exponential function, or deriving τ_h from fits to the Hodgkin–Huxley equation used above. τ_h values derived from Hodgkin–Huxley fit for both Na^+ current types showed a decrease in τ_h after PMA treatment. Mean values for τ_h in the presence and absence of PMA were 0.55 ± 0.21 msec and 0.73 ± 0.24 msec (at −10 mV, $N = 6$, $p = 0.19$) for TTX-S Na^+ currents, and 0.53 ± 0.10 msec and 0.77 ± 0.11 msec (at −30 mV, $N = 6$, $p = 0.003$) for TTX-R Na^+ currents. Surprisingly, when we used the alternate approach to derive τ_h values, namely, fitting the current decay phase only to an exponential function, we discovered that in TTX-R currents PMA altered the mode of Na^+ current inactivation from a single- to a bi-exponential decay, a phenomenon never observed in TTX-S Na^+ currents. Thus, while control TTX-R data could be fit well by a single exponential (Fig. 8*b*, control curve), the PMA data required an additional exponential with a faster time constant (Fig. 8*b*, PMA curve). Interestingly, both the amplitude and time constant of the slower inactivation time constant ($\tau_1 = 0.91$ msec; mean, 0.89 ± 0.44 msec, $N = 8$) were almost unchanged in PMA ($p = 0.72$; $\tau = 0.90$ msec; mean, 0.95 ± 0.17 msec, $N = 8$), and a second, faster time constant ($\tau_2 = 0.26$ msec; mean, 0.30 ± 0.16 msec, $N = 8$) appeared. In contrast, TTX-S Na^+ current decay could always be fit to a single exponential function (Fig. 8*a*; $N = 8$).

Discussion

Spinal cord astrocytes in culture, unlike other glial cell preparations (Sontheimer, 1992), express Na^+ channels at high densities (2–8 channels/μm^2), comparable to Na^+ channel densities in cultured neurons (Catterall, 1984; MacDermott and Westbrook, 1986; Sontheimer et al., 1991). They contain two morphological subtypes of astrocytes, which are also encountered in cultures from other brain areas, and these express biophysically and pharmacologically distinct Na^+ current types: *stellate cells* express TTX-S Na^+ currents ($K_d = 5.7$ nM) with h_∞ curve midpoints close to −60 mV; *pancake cells* express TTX-R Na^+ currents ($K_d = 1000$ nM) with h_∞ midpoints close to −85 mV (Sontheimer and Waxman, 1992b). We demonstrate here that these two Na^+ current types differ additionally in their functional modulation by PKC. TTX-S Na^+ conductances decrease at potentials more positive than −20 mV, and this decrease is associated with faster current inactivation. In contrast, TTX-R Na^+ conductances increase at all potentials and currents activate more rapidly following activation of PKC. PKC activation was induced by the phorbol ester PMA and could be inhibited by the PKC inhibitor H7 (Hidaka et al., 1984). Both current types displayed a voltage dependence in the effects of PMA. Thus, for both current types steady-state activation (*g–V*) curves were shifted toward more negative potentials following PMA treatment, resulting in enhanced conductances at activation threshold, whereas steady-state inactivation curves h_∞ were not sig-

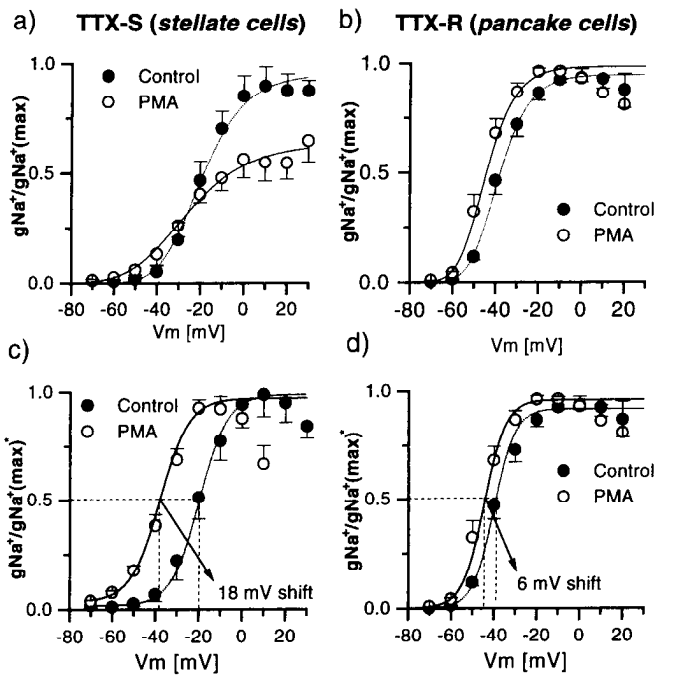

Figure 6. Voltage dependence of PMA-induced conductance changes. For five cells each of TTX-R and TTX-S Na^+ currents we derived peak conductances (g_{Na^+}) from peak currents recorded over a potential range of −70 to 30 mV in the presence (*open circles*) and absence (*solid circles*) of PMA. For each experiment, these values were normalized to the largest conductance and mean values (±SEM) of the five cells were plotted as a function of applied test potential. To illustrate the changes in conductances induced by PMA, the data were plotted as normalized g–V curves (in *a* and *b*) by normalizing conductances for each potential to the largest conductance observed irrespective of drug treatment. TTX-S conductances decreased for potentials more positive than −20 mV (*a*), whereas TTX-R conductances increased at all potentials after PMA exposure, and effects were largest between −50 and −30 mV (*b*). To illustrate the voltage dependence of PMA effects, normalized g–V curves were plotted in which conductances were normalized to the largest conductance observed for the particular recording condition (control or PMA). Curves for TTX-S (*c*) and TTX-R (*d*) currents were shifted by 18 and 6 mV, respectively, after PMA exposure. For all experiments PMA was applied for 5 min. The *continuous lines* were obtained by fitting the data to a Boltzmann function of the form $h(V) = 1/[1 + \exp(-(V - V_{1/2})/a)]$.

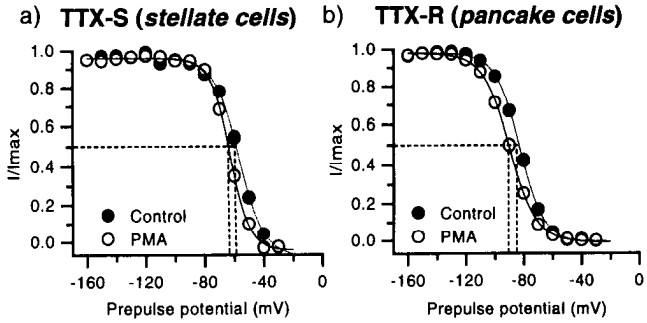

Figure 7. Effects of PMA on steady-state Na^+ current inactivation (h_∞). Steady-state inactivation curves were obtained from conditional prepulse protocols by altering prepulse potentials between −160 and −30 mV (200 msec) prior to an activating voltage step to 0 mV. Currents were normalized to the largest amplitude and mean values of five cells each for TTX-R and TTX-S were plotted as a function of prepulse potential. The data was fit to a Boltzmann equation (*continuous* and *dotted lines*) to yield h_∞ curves. These were shifted slightly but not significantly (by −3 and −5 mV; *dotted lines in c* and *d*) after a 10 min PMA exposure for both TTX-S and TTX-R. Changes in slopes were small and also not significant.

nificantly altered. The shifts in steady-state activation, however, were insufficient to account for the observed changes in peak Na^+ currents, and particularly fail to explain the different effects of PMA on TTX-S and TTX-R Na^+ currents, respectively. In addition to the effects on steady-state current parameters, PMA had differential effects on the time constants of both current activation (τ_m) and inactivation (τ_h). PMA treatment increased current activation of TTX-R Na^+ currents but did not affect τ_m in TTX-S Na^+ currents. Current inactivation (τ_h) was faster in both current types following PMA treatment, and in addition, in TTX-R Na^+ currents the inactivation changed from single to bi-exponential. We are at present unable to explain this apparent change in the mode of inactivation of TTX-R Na^+ channels. It may suggest that PMA recruits a formerly quiescent Na^+ channel population with different kinetic features, which would also explain the increase in peak currents observed. However, single-channel analysis will be essential to understand the underlying mechanism.

The effects of PMA on τ_m and τ_h of TTX-S and TTX-R Na^+ currents in astrocytes differ qualitatively from those previously reported for neuronal Na^+ channels (Lotan et al., 1990; Dascal and Lotan, 1991; Numann et al., 1991; Schreibmayer et al., 1991; Li et al., 1992). In those studies using recombinant TTX-S neuronal Na^+ channels, PKC activation always reduced peak Na^+ currents in concert with an increase in the time constant of current inactivation τ_h and a positive shift of steady-state current activation (Dascal and Lotan, 1991). Two common features were observed between astrocytic TTX-S and neuronal Na^+ channels following PKC activation: (1) in both preparations h_∞ is unaffected, and (2) currents amplitudes are reduced. In contrast to PMA effects on neuronal TTX-S channels is the decrease in τ_h and the large (−18 mV) negative shift of steady-state current activation observed in TTX-S Na^+ currents of astrocytes. These differences of PMA effects on TTX-S Na^+

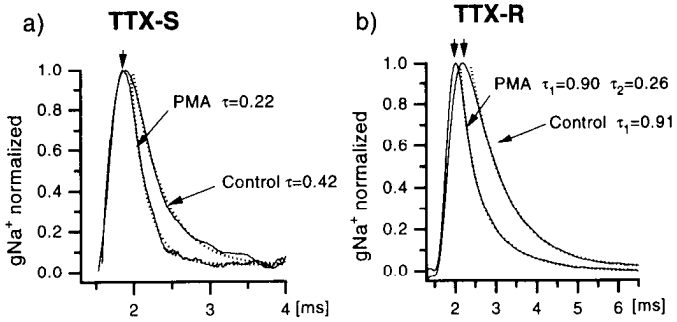

Figure 8. PMA effects on Na^+ current activation and inactivation. To asses changes to Na^+ current activation (τ_m) and inactivation (τ_h), respectively, conductances derived from current recordings in the presence and absence of PMA were plotted to scale and superimposed for both Na^+ current types. The example traces shown are representative of all other recordings, and for clarity are shown for one potential only (−10 mV for TTX-S and −30 mV for TTX-R) only. The decay phase of the currents was fit to an exponential of the form $f(t) = A_1 \cdot \exp(-(x - x_0)/\tau_1) + A_2 \cdot \exp(-(x - x_0)/\tau_2)$ (*dotted lines*). *a*, TTX-S conductances decayed with a single exponential and were altered by PMA in that τ_h decreased from 0.42 msec to 0.22 msec, while in contrast time to peak changed little (*arrows*). *b*, PMA altered both activation and inactivation kinetics of TTX-R Na^+ currents. Time to peak was reduced (*arrows*) and inactivation changed from a single exponential with a τ_h of 0.91 (at −30 mV) to a bi-exponential with time constants of $\tau_1 = 0.26$ and $\tau_2 = 0.9$ msec, respectively.

currents in astrocytes and recombinant neuronal Na^+ channels indicate that astrocytes may express an isoform of Na^+ channel not expressed in brain neurons. Neuronal TTX-R Na^+ currents are less well characterized, and modulatory roles of PKC are presently not known. However, TTX-insensitive Na^+ currents expressed in a cardiac cell line from transgenic mice have recently been demonstrated to be modulated by cAMP-dependent protein kinase (PKA) activation (Sculptoreanu et al., 1992), and may thus also be substrate for PKC modulation.

The different degree of TTX sensitivity of astrocyte Na^+ currents combined with the different steady-state activation and inactivation properties and their differential modulation by PKC strongly suggest that the two Na^+ current types, designated TTX-S and TTX-R, respectively, are meditated by different channel types, possibly differing also in their molecular structure. This notion has gained recent support from the observation that TTX sensitivity of Na^+ channels is determined by the primary amino acid sequence (Noda et al., 1989; Yang et al., 1992), although definitive proof has to await molecular cloning of the genes encoding these astrocyte Na^+ channels. A partial clone of a putative glial Na^+ channel gene (Na-G) has recently been characterized, and the amino acid sequence deduced from this cDNA indicates that Na-G represents a separate molecular class within the mammalian Na^+ channel multigene family (Gautron et al., 1992).

Since the functional role of glial Na^+ channels is not understood, the functional importance of PKC modulation of Na^+ channels in glia is likewise an enigma. The expression of Na^+ channels in glial cells *in vivo* has been controversial, and it was unclear whether glial cells *in vivo* express Na^+ channels or whether these channels are an artifact of cell culture. However, recent patch-clamp recordings from acutely isolated rat optic nerve astrocytes (Barres et al., 1990) and identified glial cells in hippocampal brain slices (Sontheimer and Waxman, 1992a) have been able to demonstrate the expression of Na^+ channels in astrocytes *in situ*, dismissing the notion that these channels are an artifact of cell culture. Ritchie and colleagues (Bevan et al., 1985) suggested that glial cells may synthesize Na^+ channel destined to be donated to neurons and axons, thus reducing their metabolic load, and immunohistochemical studies showed that astrocyte end-feet in close proximity to nodes of Ranvier express Na^+ channel immunoreactivity (Black et al., 1989). Other, more recent studies (Sontheimer, 1992; Sontheimer et al., 1993) suggest that astrocyte Na^+ channels, and in particular TTX-R Na^+ channels, may be involved in maintaining cytoplasmic Na^+ concentrations high enough to maintain the Na^+/K^+-ATPase operational.

While those roles of glial Na^+ channels are only speculative, the expression of TTX-R Na^+ channels has been demonstrated in excitable cells (Rogart et al., 1989; Cribbs et al., 1990; Kallen et al., 1990; Yang et al., 1991; Sculptoreanu et al., 1992), including central (Ikeda and Schofield, 1987) and peripheral neurons (Kostyuk et al., 1981; Caffrey et al., 1992; Roy and Narahashi, 1992) and TTX-R Na^+ currents have been implicated in the modulation of neuronal signals (French et al., 1990). If neuronal TTX-R currents are modulated in a similar fashion as described here for TTX-R Na^+ currents in astrocytes, alterations in their activity would have profound effects on their signaling behavior. Particularly, the negative shift in steady-state activation would move the threshold for current activation closer to the resting potential and would thus lower their threshold for activation.

References

Auld VJ, Goldin AL, Krafte DS, Marshall J, Dunn JM, Catterall WA, Lester HA, Davidson N, Dunn RJ (1988) A rat brain Na^+ channel alpha subunit with novel gating properties. Neuron 1:449–461.

Barchi RL (1987) Sodium channel diversity: subtle variations on a complex theme. Trends Neurosci 10:221–223.

Barres BA, Koroshetz WJ, Swartz KJ, Chun LLY, Corey DP (1990) Ion channel expression by white matter glia: the O2A glial progenitor cell. Neuron 4:507–524.

Bevan S, Chiu SY, Gray PTA, Ritchie JM (1985) The presence of voltage-gated sodium, potassium and chloride channels in rat cultured astrocytes. Proc R Soc Lond [Biol] 225:299–313.

Bezanilla F, Armstrong CM (1977) Inactivation of the sodium channel: I. Sodium current experiments. J Gen Physiol 70:549–566.

Black JA, Waxman SG, Friedman B, Elmer LW, Angelides KJ (1989) Sodium channels in astrocytes of rat optic nerve *in situ*: immunoelectron microscopic studies. Glia 2:353–369.

Black JA, Sontheimer H, Waxman SG (1993) Spinal cord astrocytes *in vitro*: sodium channel immunoreactivity. Glia 7:272–285.

Browning MD, Huganir R, Greengard P (1985) Protein phosphorylation and neuronal function. J Neurochem 45:11–23.

Caffrey JM, Eng DL, Black JA, Waxman SG, Kocsis JD (1992) Three types of sodium channels in adult rat dorsal root ganglion neurons. Brain Res 592:283–297.

Catterall WA (1984) The molecular basis of neuronal excitability. Science 223:653–661.

Catterall WA (1988) Structure and function of voltage-sensitive ion channels. Science 242:50–61.

Costa MR, Casnellie JE, Catterall WA (1982) Selective phosphorylation of the alpha subunit of the sodium channel by cAMP-dependent protein kinase. J Biol Chem 257:7918–7921.

Cribbs LL, Satin J, Fozzard HA, Rogart RB (1990) Functional expression of the heart I Na^+ channel isoform. Demonstration of properties characteristic of native cardiac Na^+ channels. FEBS Lett 275: 195–200.

Dascal N, Lotan I (1991) Activation of protein kinase C alters voltage dependence of a Na^+ channel. Neuron 6:165–175.

Dave V, Gordon GW, McCarthy KD (1991) Cerebral type 2 astroglia are heterogeneous with respect to their ability to respond to neuroligands linked to calcium mobilization. Glia 4:440–447.

Emerick MC, Agnew WS (1989) Identification of phosphorylation sites for adenosine 3′,5′-cyclic phosphate dependent protein kinase on the voltage-sensitive sodium channel from *Electrophorus electricus*. Biochemistry 28:8367–8380.

Farley J, Auerbach S (1986) Protein kinase C activation induces conductance changes in *Hermissenda* photoreceptors like those seen in associative learning. Nature 319:220–223.

French CR, Sah P, Buckett KJ, Gage PW (1990) A voltage-dependent persistent sodium current in mammalian hippocampal neurons. J Gen Physiol95:1139–1157.

Gautron S, Dossantos G, Pintohenrique D, Koulakoff A, Gros F, Berwald-Netter Y (1992) The glial voltage-gated sodium channel—cell-specific and tissue-specific messenger RNA expression. Proc Natl Acad Sci USA 89:7272–7276.

Hamill OP, Marty A, Neher E, Sakmann B, Sigworth FJ (1981) Improved patch-clamp techniques for high-resolution current recording from cells and cell-free membrane patches. Pfluegers Arch 391:85–100.

Hidaka H, Inagaki M, Kawamoto S, Sasaki Y (1984) Isoquinolinesulfonamides, novel and potent inhibitors of cyclic nucleotide dependent protein kinase and protein kinase C. Biochemistry 23:5036–5041.

Higashida H, Brown DA (1986) Two polyphosphatidylinositide metabolites control two K^+ currents in a neuronal cell. Nature 323:333–335.

Hockberger P, Toselli M, Swandulla D, Lux HD (1989) A diacylglycerol analogue reduces neuronal calcium currents independently of protein kinase C activation. Nature 338:340–342.

Hodgkin AL, Huxley AF (1952) A quantitative description of membrane current and its application to conduction and excitation in nerve. J Physiol (Lond) 117:500–544.

Ikeda SR, Schofield GG (1987) Tetrodotoxin-resistant sodium current of rat nodose neurones: monovalent cation selectivity and divalent cation block. J Physiol (Lond) 389:255–270.

Kaczmarek LK (1987) The role of protein kinase C in the regulation

of ion channels and neurotransmitter release. Trends Neurosci 10: 30–34.
Kallen RG, Sheng Z-H, Yang J, Chen L, Rogart RB, Barchi RL (1990) Primary structure and expression of a sodium channel characteristic of denervated and immature skeletal muscle. Neuron 4:233–242.
Kostyuk PG, Veselovsky NS, Tsyndrenko AY (1981) Ionic currents in the somatic membrane of rat dorsal root ganglion neurons. I. Sodium currents. Neuroscience 6:2423–2430.
Lemos JR, Novak-Hofer I, Levitan IB (1986) Regulation of ion channel activity by protein phosphorylation. Prog Brain Res 69:107–118.
Levitan IB (1988) Modulation of ion channels in neurons and other cells. Annu Rev Neurosci 11:119–136.
Levitan IB, Chung S, Reinhart PH (1990) Modulation of a single ion channel by several different protein kinases. Adv Second Messenger Phosphoprotein Res 24:36–40.
Li M, West JW, Lai Y, Scheuer T, Catterall WA (1992) Functional modulation of brain sodium channels by cAMP-dependent phosphorylation. Neuron 8:1151–1159.
Lotan I, Dascal N, Naor Z, Boton R (1990) Modulation of vertebrate brain Na^+ and K^+ channels by subtypes of protein kinase C. FEBS Lett 267:25–28.
MacDermott AB, Westbrook GL (1986) Early development of voltage-dependent sodium currents in cultured mouse spinal cord neurons. Dev Biol 113:317–326.
Madison DV, Malenka RC, Nicoll RA (1986) Phorbol esters block a voltage-sensitive chloride current in hippocampal pyramidal cells. Nature 321:695–697.
Malenka RC, Madison DV, Nicoll RA (1986) Potentiation of synaptic transmission in the hippocampus by phorbol esters. Nature 321:175–177.
Marty A, Neher E (1983) Tight-seal whole-cell recording. In: Single-channel recording (Sakmann B, Neher E, eds), pp 107–122. New York: Plenum.
McLean MJ, Bennett PB, Thomas RM (1988) Subtypes of dorsal root ganglion neurons based on different inward currents as measured by whole-cell voltage-clamp. Mol Cell Biochem 80:95–107.
Miller RH, Szigeti V (1991) Clonal analysis of astrocyte diversity in neonatal rat spinal cord cultures. Development 113:353–362.
Nairn AC, Hemmings HJ, Greengard P (1985) Protein kinases in the brain. Annu Rev Biochem 54:931–976.
Nishizuka Y (1984) Turnover of inositol phospholipids and signal transduction. Science 225:1365–1370.
Noda M, Shimizu S, Tanabe T, Takai T, Kayano T, Ikeda T, Takahashi H, Nakayama H, Kanaoka Y, Minamino N, Kangawa K, Matsuo H, Raftery MA, Hirose T, Inayama S, Hayashida H, Miyata T, Numa S (1984) Primary structure of *Electrophorus electricus* sodium channel deduced from cDNA sequence. Nature 312:121–127.
Noda M, Suzuki H, Numa S, Stühmer W (1989) A single point mutation confers tetrodotoxin and saxotoxin insensitivity on the sodium channel II. FEBS Lett 259:213–216.
Numann R, Catterall WA, Scheuer T (1991) Functional modulation of brain sodium channels by protein kinase C phosphorylation. Science 254:115–118.
Raff MC (1989) Glial cell diversification in the rat optic nerve. Science 243:1450–1455.
Rane SG, Dunlap K (1986) Kinase C activator 1,2-oleoylacetylglycerol attenuates voltage-dependent calcium current in sensory neurons. Proc Natl Acad Sci USA 83:184–188.
Rogart RB, Cribbs LL, Muglia LK, Kephart DD, Kaiser MW (1989) Molecular cloning of a putative tetrodotoxin-resistant rat heart Na^+ channel isoform. Proc Natl Acad Sci USA 86:8170–8174.
Rossie S, Catterall WA (1989) Phosphorylation of the alpha subunit of rat brain sodium channels by cAMP-dependent protein kinase at a new site containing Ser^{686} and Ser^{687}. J Biol Chem 264:14220–14224.
Roy ML, Narahashi T (1992) Differential properties of tetrodotoxin-sensitive and tetrodotoxin-resistant sodium channels in rat dorsal root ganglion neurons. J Neurosci 12:2104–2111.
Schmidt J, Rossie S, Catterall WA (1985) A large intracellular pool of inactive Na channel alpha subunits in developing rat brain. Proc Natl Acad Sci USA 82:4847–4851.
Schreibmayer W, Dascal N, Lotan I, Wallner M, Weigl L (1991) Molecular mechanism of protein kinase C modulation of sodium channel alpha-subunits expressed in *Xenopus* oocytes. FEBS Lett 291:341–344.
Schwartz A, Palti Y, Meivi H (1990) Structural and developmental difference between three types of Na^+ channels in dorsal root ganglion cells of newborn rats. J Membr Biol 116:117–128.
Sculptoreanu A, Morton M, Gartside CL, Hauschka SD, Catterall WA, Scheuer T (1992) Tetrodotoxin-insensitive sodium channels in a cardiac cell line from a transgenic mouse. Am J Physiol 31:C724–C730.
Sigel E, Baur R (1988) Activation of protein kinase C differentially modulates neuronal Na^+, Ca^{2+}, and gamma-aminobutyrate type A channels. Proc Natl Acad Sci USA 85:6192–6196.
Sontheimer H (1992) Astrocytes, as well as neurons, express a diversity of ion channels. Can J Physiol Pharmacol 70:s223–s238.
Sontheimer H, Waxman SG (1992a) Glial cells *in situ* in hippocampal slices express voltage-activated Na^+ and K^+ channels. Soc Neurosci Abstr 18:64.
Sontheimer H, Waxman SG (1992b) Ion channels in spinal cord astrocytes *in vitro*: II. Biophysical and pharmacological analysis of two Na^+ current types. J Neurophysiol 68:1001–1011.
Sontheimer H, Ransom BR, Cornell-Bell AH, Black JA, Waxman SG (1991) Na^+-current expression in rat hippocampal astrocytes *in vitro*: alterations during development. J Neurophysiol 65:3–19.
Sontheimer H, Black JA, Ransom BR, Waxman SG (1992) Ion channels in spinal cord astrocytes *in vitro*: I. Transient expression of high levels of Na^+ and K^+ channels. J Neurophysiol 68:985–1000.
Sontheimer H, Fernandez E, Ullrich N, Waxman SG (1993) Glial Na^+ channel are required for maintenance of Na^+/K^+-ATPase activity. Soc Neurosci Abstr, in press.
Strichartz G, Rando T, Wang GK (1987) An integrated view of the molecular toxinology of sodium channel gating in excitable cells. Annu Rev Neurosci 10:237–267.
West JW, Numann R, Murphey BJ, Scheuer T, Catterall WA (1991) A phosphorylation site in the Na^+ channel is required for modulation by protein kinase C. Science 254:866–868.
Wyllie DJA, Mathie A, Symonds CJ, Cull-Candy SG (1991) Activation of glutamate receptors and glutamate uptake in identified macroglial cells in rat cerebellar cultures. J Physiol (Lond) 432:235–258.
Yang JS-J, Sladky JT, Kallen RG, Barchi RL (1991) TTX-sensitive and TTX-insensitive sodium channel mRNA transcripts are independently regulated in adult skeletal muscle after denervation. Neuron 7:421–427.
Yang XC, Labarca C, Nargeot J, Ho BY, Elroy SO, Moss B, Davidson N, Lester HA (1992) Cell-specific posttranslational events affect functional expression at the plasma membrane but not tetrodotoxin sensitivity of the rat brain IIA sodium channel alpha-subunit expressed in mammalian cells. J Neurosci 12:268–277.